©SNAK, 2015

Int. J. Nav. Archit. Ocean Eng. (2015) 7:478~489
http://dx.doi.org/10.1515/ijnaoe-2015-0034
pISSN: 2092-6782, eISSN: 2092-6790

Hull-form optimization of a container ship based on bell-shaped modification function

Hee Jong Choi

Department of Naval Architecture and Ocean Engineering, Chonnam National University, Yeosu, Korea

Received 21 February 2013; Revised 26 November 2013; Accepted 13 February 2015

ABSTRACT: *In the present study, a hydrodynamic hull-form optimization algorithm for a container ship was presented in terms of the minimum wave-making resistance. Bell-shaped modification functions were developed to modify the original hull-form and a sequential quadratic programming algorithm was used as an optimizer. The wave-making resistance as an objective function was obtained by the Rankine source panel method in which non-linear free surface conditions and the trim and sinkage of the ship were fully taken into account. Numerical computation was performed to investigate the validity and effectiveness of the proposed hull-form modification algorithm for the container carrier. The computational results were validated by comparing them with the experimental data.*

KEY WORDS: Hydrodynamic hull-form optimization; Bell-shaped modification function; Sequential quadratic programming (SQP); Container carrier; Rankine source panel method.

INTRODUCTION

The fundamental elements of a hydrodynamic hull-form optimization technique consist of an optimizer, a numerical solver and a hull-form modification.

As an optimizer, gradient-based optimization technique has been widely used because of fast convergence. The Non-Linear Programming (NLP) technique has been principally challenging various gradient-based optimization techniques. SQP algorithm that uses an active set strategy in solving Quadratic Programming (QP) and QP sub-problems proves to be efficient in locating the points of local optima and the most successful method for solving non-linearly constrained optimization problems.

As a numerical solver for finding the ship resistance which is used as an objective function in the optimization process, the Navier-Stokes solver should be applied to take viscous effects into account. However this approach consumes excessive computation time in generating computational grid and numerical computation and faster and more reasonable approach therefore need to be available in the practical stage. A potential flow solver based on the Rankine source panel method has been widely applied as an alternative to the Navier-Stokes solver. The hull-form optimization were performed applying the Rankine source panel method to achieve the wave-making resistance as the objective function focusing on the optimization of the bow-body shape (Suzuki et al., 2005; Zhang et al., 2009; Zhang, 2012).

A hull-form modification technique is very important in hydrodynamic hull-form optimization. During the optimization process, we only need to modify the original hull-form, which is called the mother ship, and the development of an efficient

Corresponding author: *Hee Jong Choi*, e-mail: *choihj@jnu.ac.kr*

hull-form modification technique for the mother ship is essential in order to make the optimization process efficient and practical.

Three principal approaches have been widely used in hull-form modification (Chen et al., 2006; Han et al., 2012; Maisonneuve et al., 2003; Peri et al., 2005; Tahara et al., 2004; Tahara et al., 2006).

The first approach, which originated from ship designers in yards, is to use parametric modeling where the original hull geometry can be easily deformed as well as modeled by a direct selection of design parameters. This method is very practical for designers since the parametric modeling can be easily linked to the optimization process. However, it is difficult to describe highly complex geometries of a modern commercial ship with all of the form parameters.

The second approach is to directly handle the original hull-form by modifying a ship lines which consists of a body plan, a sheer plan and a half breadth plan. However, this method requires a great deal of computation time in the optimization process and has a critical drawback in that the fairness of the generated hull-form cannot always be guaranteed.

The third approach is to use perturbation surfaces generated by modification functions such as B-spline and Bezier techniques. This method is much improved from the second approach in terms of computation time and the fairness of the generated hull-form and has been successfully employed for the optimization of commercial ships. However, this approach needs a few of control vertex to describe the original hull-form and difficult to maintain the ship-like shape of the modified hull-form during the optimization process and a great deal of computation time is required because of a lot of design variables.

In the present study, a bell-shape modification function was developed in order to solve the problems of previous researches. This approach could use a small number of design variables to modify the hull-form and easy to maintain the ship-like shape of the modified hull during the optimization process. *SQP* was used as an optimizer and the Rankine source panel method was adopted to compute the objective function in which the fully non-linear free surface condition and the trim and sinkage of the ship were taken into account. Numerical analysis was performed to investigate the validity of the proposed algorithm using a container ship. The numerical analysis was validated by comparison with the experimental analysis.

BELL-SHAPED MODIFICATION FUNCTION

The bell-shaped modification functions are applied to modify the original hull in the optimization process. The original hull is modified by multiplying the functions and design variables. The design variables represent the moving distance of the specific coordinates which is selected by the user.

Two types of the bell-shaped modification functions are applied to modify the hull profile and the hull surface as shown in Figs. 1 and 2.

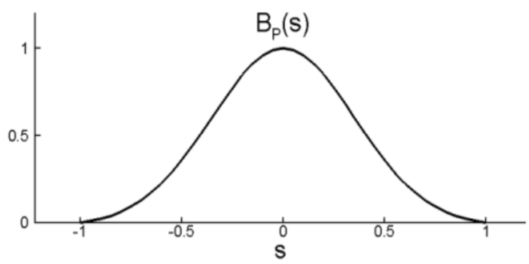

Fig. 1 Bell-shaped modification function for modifying the hull profile.

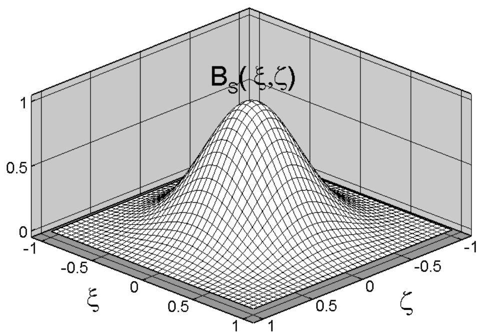

Fig. 2 Bell-shaped modification function for modifying the hull surface.

The bell-shaped modification function for modifying the hull profile is defined as

$$B^{P}_{i,i_P}(s) = e^{-4s^2} - |s|e^{-4} \tag{1}$$

$$
\begin{aligned}
s &= 2\sum_{k=i}^{i_P-1} \sqrt{(x_{k+1}-x_k)^2+(z_{k+1}-z_k)^2} \,/\, s_{\max}\,, \quad i \le i_P \\
s &= 2\sum_{k=i_P}^{i-1} \sqrt{(x_{k+1}-x_k)^2+(z_{k+1}-z_k)^2} \,/\, s_{\max}\,, \quad i > i_P
\end{aligned} \tag{2}
$$

$$
s_{\max} = \sum_{k=1}^{NP-1} \sqrt{(x_{k+1}-x_k)^2+(z_{k+1}-z_k)^2} \tag{3}
$$

The modified hull profile is expressed mathematically as

$$
\begin{aligned}
x_i^n &= x_i^o + \sum_{k=1}^{NX} \alpha_k^x \, B_{i,i_k}^P\,, \quad i=1,\dots,NP \\
z_i^n &= z_i^o + \sum_{k=1}^{NZ} \alpha_k^z \, B_{i,i_k}^P\,, \quad i=1,\dots,NP
\end{aligned} \tag{4}
$$

In Eq. (4), α^x and α^z represent moving distance of x_k and z_k respectively, which is used as design variables during the optimization process as shown in Fig. 3.

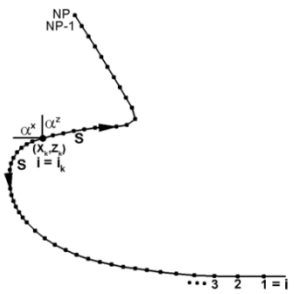

Fig. 3 Description of design variables and parametric distance (s) for modifying the hull profile.

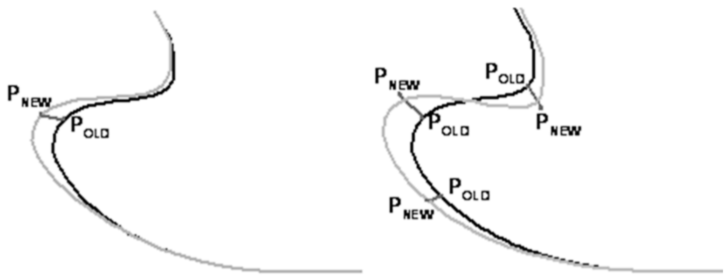

Fig. 4 Original hull profile and modified hull profile after applying two (left) and six (right) design variables.

Fig. 4 shows the fore part of the hull profile which is modified by two (one) or six (three) design variables (points). After the hull profile is modified, the grid points making up the hull surface should be transformed according to the modified hull profile.

The transformation of the hull surface is attained by the use of the following formulas

$$
\begin{aligned}
x_{i,j}^* &= x_{i,j}^o + \left(1-C_\xi\right)(x_{1,j}^n - x_{1,j}^o) + C_\xi\,(x_{n\xi,j}^n - x_{n\xi,j}^o) \\
x_{i,j}^n &= x_{i,j}^* + \left(1-C_\zeta\right)(x_{i,1}^n - x_{i,1}^*) + C_\zeta\,(x_{i,n\zeta}^n - x_{i,n\zeta}^*)
\end{aligned} \tag{5}
$$

$$
\begin{aligned}
z_{i,j}^* &= z_{i,j}^o + \left(1-C_\xi\right)(z_{1,j}^n - z_{1,j}^o) + C_\xi\,(z_{n\xi,j}^n - z_{n\xi,j}^o) \\
z_{i,j}^n &= z_{i,j}^* + \left(1-C_\zeta\right)(z_{i,1}^n - z_{i,1}^*) + C_\zeta\,(z_{i,n\zeta}^n - z_{i,n_\zeta}^*)
\end{aligned} \tag{6}
$$

$$
\begin{aligned}
C_\xi &= (e^{\xi_{i,j}} - 1)/(e-1) \\
C_\zeta &= (e^{\zeta_{i,j}} - 1)/(e-1)
\end{aligned} \tag{7}
$$

$$
\begin{aligned}
\xi_{1,j} &= 0 \\
\xi_{i,j} &= \xi_{i-1,j} + \sqrt{(x_{i,j}^o - x_{i-1,j})^2 + (z_{i,j}^o - z_{i-1,j}^o)^2} \\
\xi_{i,j} &= \xi_{i,j} \,/\, \xi_{n\xi,j}
\end{aligned} \tag{8}
$$

$$\begin{aligned}&\zeta_{i,1}=0\\&\zeta_{i,j}=\zeta_{i,j-1}+\sqrt{(x^o_{i,j}-x^o_{i,j-1})^2+(z^o_{i,j}-z^o_{i,j-1})^2}\\&\zeta_{i,j}=\zeta_{i,j}/\zeta_{i,n\zeta}\end{aligned}\tag{9}$$

The bell-shaped modification function which modifies the hull surface is defined as follows

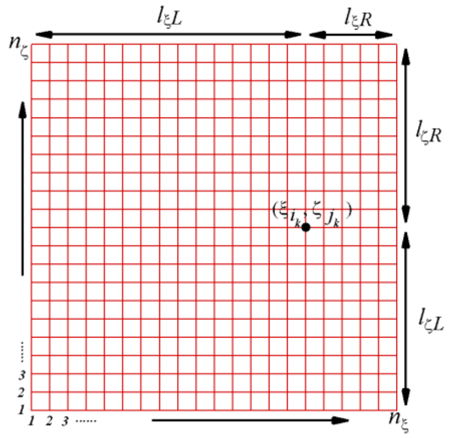

Fig. 5 Rectangular grid and description of bell-shaped modification function.

$$B^T_{(i,j),(i_k,j_k)}(u,v)=\left[e^{-4u^2}-|u|e^{-4}\right]\left[e^{-4v^2}-|v|e^{-4}\right]\tag{10}$$

$$u=\begin{cases}(\xi_{i,j}-\xi_{i_k,j_k})/l_{\xi L}\,,\ \xi_{i,j}\le\xi_{i_k,j_k}\\(\xi_{i,j}-\xi_{i_k,j_k})/l_{\xi R}\,,\ \xi_{i,j}>\xi_{i_k,j_k}\end{cases}\tag{11}$$

$$v=\begin{cases}(\zeta_{i,j}-\zeta_{i_k,j_k})/l_{\zeta L}\,,\ \zeta_{i,j}\le\zeta_{i_k,j_k}\\(\zeta_{i,j}-\zeta_{i_k,j_k})/l_{\zeta R}\,,\ \zeta_{i,j}>\zeta_{i_k,j_k}\end{cases}\tag{12}$$

$$\begin{aligned}&\xi_{1,j}=0\\&\xi_{i,j}=\xi_{i-1,j}+\sqrt{(x^o_{i,j}-x_{i-1,j})^2+(y^o_{i,j}-y^o_{i-1,j})^2+(z^o_{i,j}-z^o_{i-1,j})^2}\\&\xi_{i,j}=\xi_{i,j}/\xi_{n\xi,j}\end{aligned}\tag{13}$$

$$\begin{aligned}&\zeta_{i,1}=0\\&\zeta_{i,j}=\zeta_{i,j-1}+\sqrt{(x^o_{i,j}-x^o_{i,j-1})^2+(y^o_{i,j}-y^o_{i,j-1})^2+(z^o_{i,j}-z^o_{i,j-1})^2}\\&\zeta_{i,j}=\zeta_{i,j}/\zeta_{i,n\zeta}\end{aligned}\tag{14}$$

In Eqs. (10-14), ξ_{i_k,j_k} and ζ_{i_k,j_k} are the positions of the design variable in the rectangular grid as shown in Fig. 4. In the horizontal direction, $l_{\xi L}$ is the length between ξ_{1,j_k} and ξ_{i_k,j_k} and $l_{\xi R}$ is the length between ξ_{i_k,j_k} and $\xi_{n\xi,j_k}$. In the vertical direction, $l_{\zeta L}$ is the length between $\zeta_{i_k,1}$ and ζ_{i_k,j_k} and $l_{\zeta R}$ is the length between ζ_{i_k,j_k} and $\zeta_{i_k,n\zeta}$.

The bell-shaped modification function is transformed depending on the position of the design variable and the boundaries of the rectangular grid do not change because it has zero value at the boundaries as shown in Figs. 4 and 5. The rectangular grid could be directly mapped onto the grid which defines the hull surface since the optimization region is represented by a structured grid.

The grid points representing the surface of the modified hull are expressed mathematically as follows

$$y_{i,j}^{n} = y_{i,j}^{o} + \sum_{k=1}^{NT} \alpha_{i_k,j_k}^{T} \; B_{(i,j),(i_k,j_k)}^{T}(u,v) \tag{15}$$

α^{T} : design variable varying in only the y-direction (scalar)

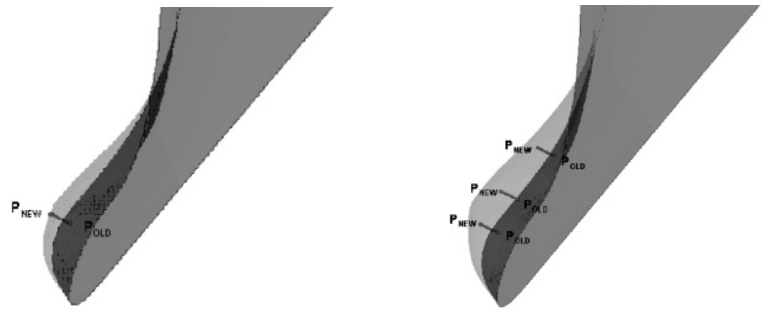

Fig. 6 Original hull and modified hull after applying one (left) and three (right) design variables.

Fig. 6 shows the modified grids when one and three design variables are applied. As shown in Figs. 4 and 6, the bell-shaped modification function is very efficient because the small number of design variables makes it possible to modify the original hull and the surface fairness of the modified hull is also excellent.

The modified hull is expressed in general form as follows:

$$(x^{n}, y^{n}, z^{n}) = (x^{o}, y^{o}, z^{o}) + \sum_{k=1}^{N} \alpha_{k} \; B \tag{16}$$

(x^{o}, y^{o}, z^{o}) : geometry of the original hull
(x^{n}, y^{n}, z^{n}) : geometry of the modified hull
B : bell-shaped modification function
α : design variable (scalar)
$N(= NX + NZ + NT)$: number of the design variables

OBJECTIVE FUNCTION

In the lack of knowledge of viscosity of the fluid and wave breaking, the irrotationality of the incoming flow is preserved and a potential flow may be assumed, in which the velocity vector is defined as the gradient of a velocity potential (ϕ). The velocity potential is governed by the Laplace equation as the fluid is assumed to be incompressible.

$$\nabla^{2}\phi = 0 \quad \text{in the fluid region} \tag{17}$$

Over the wetted part of the hull surface, the fluid particle should not penetrate the hull surface and the normal component of the flow velocity on the hull surface should be zero

$$\phi_{n} = 0 \quad \text{on the hull surface} \tag{18}$$

n : unit normal vector.

On the free surface, the flow velocity must be tangential to the free surface, which means that the flow particle at the free surface should not leave the free surface

$$\phi_x h_x + \phi_y h_y - \phi_z = 0 \quad \text{on the free surface} \tag{19}$$

h : wave elevation.

The pressure on the free surface, which is expressed in the flow velocities and wave elevation through Bernoulli's law, should be constant at the free surface

$$gh + \frac{1}{2}\left(\phi_x^2 + \phi_y^2 + \phi_z^2 - U^2 \right) = 0 \quad \text{on the free surface} \tag{20}$$

U : speed of the ship

The disturbance due to the ship approaches zero and the velocity potential should be the same as the incoming velocity potential as the distance from the ship approaches infinity.

$$\nabla\phi = \left(U,\ 0,\ 0\right) \quad \text{as} \quad x \to -\infty \tag{21}$$

Since Eqs. (19)-(20) are fully non-linear, the iterative method was used to solve the free surface problem based on the Rankine source panel method.

Having obtained the velocity potential and hence the flow velocity, the pressure coefficient ($C_{PRES.}$) at each panel can be found using Bernoulli's equation

$$C_{PRES.} = 1 - \frac{\nabla\phi \bullet \nabla\phi}{U^2} - 2\frac{z}{Fn^2} \tag{22}$$

Fn : Froude number

The wave-making resistance coefficient (C_W) is hence given by the integration of the pressure coefficient over the wetted hull surface and used as the objective function in this optimization problem (Choi et al., 2011; Raven, 1996).

$$C_W = -\frac{\int_{S_{WET}} C_{PRES.}\, n_x\, ds}{S_{WET}} \tag{23}$$

S_{WET} : wetted surface of the ship
n_x : x-component of the unit vector normal to the hull surface

OPTIMIZATION ALGORITHM

The purpose of an optimization process is to obtain the values of a set of design variables ($\alpha = [\alpha_1, \alpha_2, \alpha_3, \cdots, \alpha_N]$) that determine the optimized value of an objective function. The general optimization problem may be expressed in the following form:

Minimize:

$$f(\alpha) = C_W \tag{24}$$

Subjected to:

$$h_j(\alpha) = 0\,, \quad j = 1\,, \cdots, m_e \tag{25}$$

$$g_j(\alpha) \leq 0\,, \quad j = m_e + 1\,, \cdots,\, m \tag{26}$$

$$\alpha_l \leq \alpha \leq \alpha_u \tag{27}$$

The objective function (f) is the function of design variables under the equality constraint (h) and inequality constraint (g). The upper bound (α_u) and the lower bound (α_l) are also enforced onto the design variables.

SQP is an efficient, gradient-based, local optimization algorithm. The method has a theoretical basis that is related to the solution of a set of non-linear equations using Newton's method, and the derivation of simultaneous non-linear equations using Karush-Kuhn-Tucker conditions to the Lagrangian of the constrained optimization problem. The equations are approximated with a quadratic form:

Minimize:

$$\tfrac{1}{2} d^T B d + \nabla f(\alpha)^T d \tag{28}$$

Subject to:

$$h_j(\alpha)^T\, d + h_j(\alpha) = 0\,, \quad j = 1\,, \cdots, m_e \tag{29}$$

$$g_j(\alpha)^T\, d + g_j(\alpha) = 0\,, \quad j = m_e + 1\,, \cdots,\, m \tag{30}$$

$$\alpha_l \leq \alpha \leq \alpha_u \tag{31}$$

In Eqs. (28)-(31), d is the search direction vector and B is the approximate Hessian matrix of the Lagrangian. During the optimization process, the optimum d is determined and α is updated by $\alpha_{n+1} = \alpha_n + d$ in each iteration step.

APPLICATION

The hull-form optimization technique proposed above was applied to a container ship in order to improve the resistance performance.

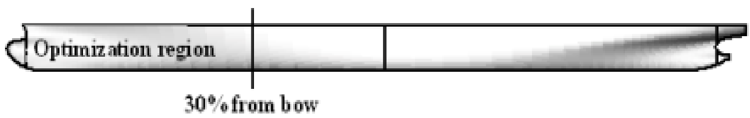

Fig. 7 Optimization region.

The hull-form optimization was only performed in the region 30% from station 14 to the bulb tip as shown in Fig. 7.

Figs. 8 and 9 show design variables. Fig. 8 shows the design variables which were applied for the profile modification and should only be moved in the bar in the horizontal or the vertical direction. Fig. 9 shows the design variables which were applied for the hull surface modification and should only be moved in the transverse direction.

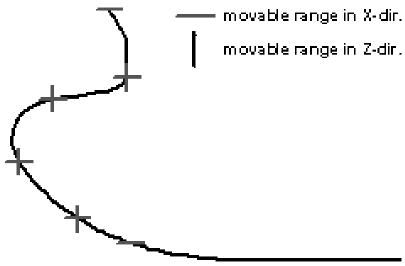

Fig. 8 Distribution of design variables for the modification of the hull profile and the movable range of the design variables.

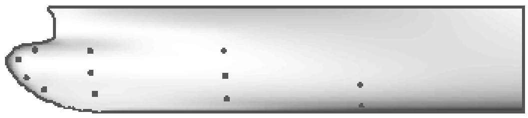

Fig. 9 Distribution of design variables for the modification of the hull surface.

Eq. (32) represents lower and upper limits of the design variables.

$$\alpha_i - 0.003 < \alpha_i < \alpha_i + 0.003 \tag{32}$$

The displacement (Δ_{SHIP}) and the wetted surface Area (S_{WET}) of the ship are important factors in ship design and the reduction in the resistance could be achieved by the decreased displacement and the decreased wetted surface area. In the present study, constraint conditions were applied to the displacement and the wetted surface area.

$$\Delta_{SHIP_{OPTIMIZED}} \geq \Delta_{SHIP_{ORIGINAL}} \tag{33}$$

$$\left| S_{WET_{OPTIMIZED}} - S_{WET_{ORIGINAL}} \right| \leq 1\% \tag{34}$$

Numerical Results

Numerical analysis for the hull-form optimization was carried out at design speed ($Fn = 0.254$).

Table 1 Comparison of the main dimensions.

	Original	Optimized	∆(%)
L_{BP}	246	246.37	0.15
B		32.25	
T		10.80	
C_B	0.6351	0.6367	0.25
S_{WET}	9852	9883	0.31
Displacement	54419	54640	0.41

The main dimensions of the original hull are compared with the optimized hull in the Table 1. It can be seen in the Table 1 that the main dimensions of the optimized hull are generally increased compared with the original hull.

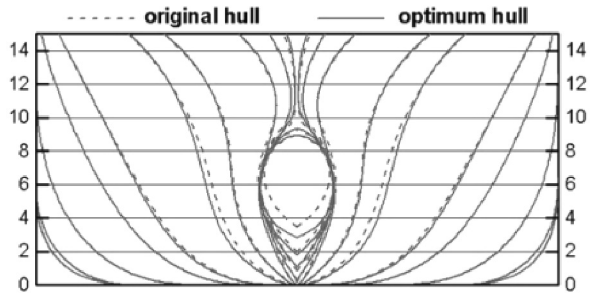

Fig. 10 Comparison of the body plans.

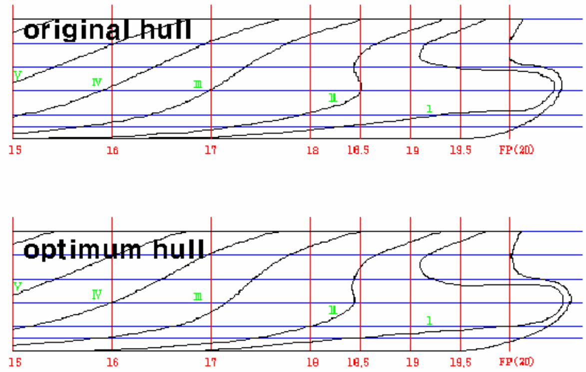

Fig. 11 Comparison of the buttock lines.

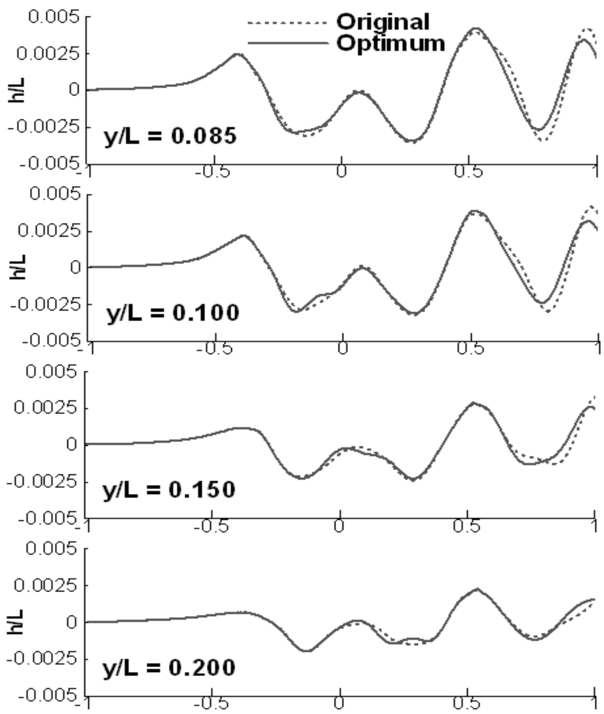

Fig. 12 Comparison of the longitudinal wave cuts.

The body plans and the buttock lines of the original hull and the optimized hull are shown in Figs. 10 and 11. The bulb of the optimized hull is sharper and larger than that of the original hull. The hull surface of the optimized hull shows enough fairness without extra fairing work.

Fig. 12 show the comparison of wave heights calculated at y/L=0.85, 1.00, 0.15 and 0.200 between the original hull and the optimized hull.

Experimental verification

The model test was carried out in a towing basin at Pusan National University in South Korea which has a length of 100 *m* and the width is 8 *m* and the depth is 3.5 *m*.

The resistance performance test and self-propulsion test were performed.

Fig. 13 Comparison of models.

Fig. 13 shows the model hulls of the original hull and the optimized hull. During the towing basin experiment studs were attached to the hull surface as turbulence simulators in the middle of the bulbous bow and the trim and sinkage of the models were taken into account. Table 2 shows the main measurements of the original hull and the optimized hull. The conversion from the model to the ship was made according to the 1978 ITTC performance prediction method. The form factor (*1+k*) was determined by Prohaska's method.

Table 2 and Fig. 14 show the comparison of the results of the resistance performance test between the original hull and the optimized hull. As shown in Table 2 and Fig. 14, residual resistance coefficient (C_R) which was measured by the model test, was reduced about 39% at the design speed and C_W which was calculated by the numerical analysis, was reduced about 27% and total resistance coefficient of the model (C_{TM}) was reduced 3% and effective horse power (EHP) is reduced 4.6%.

Table 2 Comparison of EHP .

	Original	Optimized	△ (%)
Scale factor (λ)		40	
$1+k$	1.155	1.159	
$C_{TM}\times10^3$ (exp.)	3.869	3.755	-3.0
$C_W\times10^3$ (cal.)	0.482	0.352	-26.9
$C_R\times10^3$ (exp.)	0.315	0.192	-38.9
EHP (HP)	28581	27263	-4.6

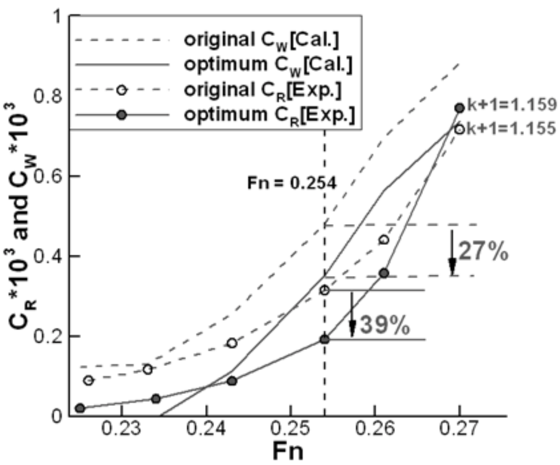

Fig. 14 Comparison of C_W or C_R.

The self-propulsion test was carried out to confirm the speed increase according to the reduction of resistance as shown in Table 3 and Figs. 15 and 16. Table 3 shows the comparisons of propulsive efficiencies and brake horse power (BHP) at the design speed.

Quasi-propulsive efficiency (η_D) and other efficiencies (i.e. hull efficiency (η_H) ; relative rotative efficiency (η_R) ; propeller efficiency (η_O)) for the optimized hull were similar to those of the original hull since the stern part of the ship was not modified during the optimization process.

BHP was therefore reduced by about 4.6%, which was similar to the reduction of EHP . The speed of the original hull was 24.51 *knots* and the speed of the optimized hull was 24.74 *knots* for normal continuous rating (NCR) power. The reduction of resistance according to the hull-form optimization brought the speed up to about 0.23 *knots* with the same power. Fig. 16 shows the comparison of BHP .

Table 3 Comparison of η_H , η_R , η_O , η_D and BHP .

	original	optimized	Δ(%)
η_H	1.081	1.090	0.8
η_R	1.013	0.990	-2.3
η_O	0.638	0.642	0.6
η_D	0.698	0.693	-0.7
BHP (HP)	41277	39365	-4.6
Speed / RPM for NCR	24.51 *knots* / 97.4 *rpm*	24.74 *knots* / 97.4 *rpm*	0.23 *knots*

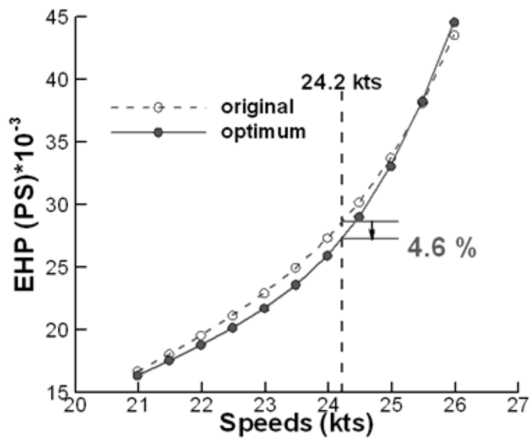

Fig. 15 Comparison of EHP .

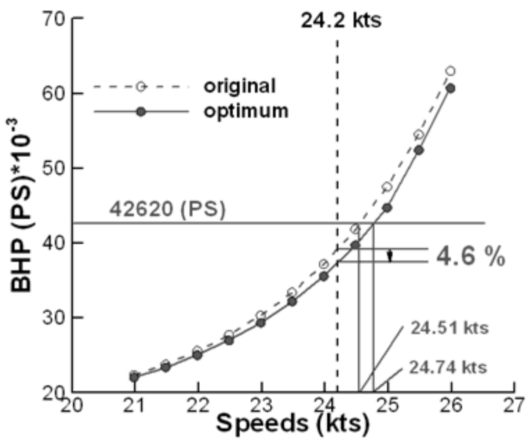

Fig. 16 Comparison of BHP .

CONCLUSIONS

In the present study, the bell-shaped modification function was developed to efficiently modify the hull-form of the ship during the hull-form optimization process. The hull-form optimization algorithm adopting the developed method was applied to the container carrier in terms of the minimum wave-making resistance. The model test was performed to validate the adopted method and the results obtained by numerical analysis were compared with the experimental data.

The comparison between experimental and numerical analysis shows that the proposed bell-shaped modification functions are very efficient because the small number of design variables makes it possible to modify the original hull and the surface fairness of the modified hull is consistently excellent during the optimization process. The adopted optimization algorithm is proven to be applicable to search for the optimized hull-form. Further study on several types of ships is recommended in future work.

REFERENCES

Chen, P.F., Huang, C.H., Fang, M.C. and Chou, J.H., 2006. An inverse design approach in determining the optimal shape of bulbous bow with experimental verification. *Journal of Ship Research*, 50(1), pp.1-14.

Choi, H.J., Chun, H.H., Park, I.L. and Kim, J., 2011. Panel cutting method: new approach to generate panels on a hull in rankine source potential approximation. *International Journal of Naval Architecture and Ocean Engineering*, 3(4), pp.225-232.

Han, S.H., Lee, Y.S. and Choi, Y.B., 2012. Hydrodynamic hull form optimization using parametric models. *Journal of Marine Science and Technology*, 17(1), pp.1-17.

Maisonneuve, J.J., Harries. S., Marzi, J., Raven, H.C., Viviani, U. and Piippo, H., 2003. Towards optimal design of ship hull shapes. *Proceedings of the 8th International Marine Design Conference IMDC'03*, Athens, Greece, 3-5 June 2003, pp.31-42.

Peri, D. and Campana, E.F., 2005. High-fidelity models and multiobjective global optimization algorithms in simulation-based design. *Journal of Ship Research*, 49(3), pp.159-175.

Raven, H.C., 1996. *A solution method for the nonlinear ship wave resistance problem*. Ph.D. Thesis. Delft University, Netherlands.

Suzuki, K., Kai, H. and Kashiwabara, S., 2005. Studies on the optimization of stern hull-form based on a potential flow solver. *Journal of Marine Science and Technology*, 10(2), pp.61-69.

Tahara, Y., Stern, F. and Himeno, Y., 2004. Computational fluid dynamics-based optimization of surface combatant. *Journal of Ship Research*, 48(4), pp.273-287.

Tahara, Y., Tohyama, S. and Katsui, T., 2006. CFD-based multi-objective optimization method for ship design. *International Journal for Numerical Methods in Fluids*, 52(5), pp.499-527.

Zhang, B.J., 2012. Research on optimization of hull lines for minimum resistance based on rankine source method. *Journal of Marine Science and Technology*, 20(1), pp.89-94.

Zhang, B.J., Ma, K and Ji, Z. S., 2009. The optimization of the hull-form with the minimum wave making resistance based on rankine source method. *Journal of Hydrodynamics, Series B,* 21(2), pp.277-284.